Available online at www.sciencedirect.com
SCIENCE DIRECT
Journal of Solid State Chemistry 179 (2006) 935–940
JOURNAL OF SOLID STATE CHEMISTRY
www.elsevier.com/locate/jssc

Single-crystal growth of $Tl_2Ru_2O_7$ pyrochlore using high-pressure and flux method

Daisuke Mori[a], Noriyuki Sonoyama[a], Atsuo Yamada[a], Ryoji Kanno[a,*], Masaki Azuma[b], Mikio Takano[b], Katsumi Suda[c], Nobuo Ishizawa[d]

[a]*Department of Electronic Chemistry, Interdisciplinary Graduate School of Science and Engineering, Tokyo Institute of Technology, Midori-ku, Yokohama, Kanagawa 226-8502, Japan*
[b]*Institute for Chemical Research, Kyoto University, Uji, Kyoto-fu 611-0011, Japan*
[c]*Materials and Structures Laboratory, Tokyo Institute of Technology, Midori-ku, Yokohama, Kanagawa 226-8502, Japan*
[d]*Ceramics Research Laboratory, Nagoya Institute of Technology, Tajimi, Gifu 507-0071, Japan*

Received 14 September 2005; received in revised form 22 November 2005; accepted 11 December 2005
Available online 20 January 2006

Abstract

Single crystals of the thallium ruthenium pyrochlore have been grown by flux method under high oxygen pressure. The growth conditions were determined by direct observations using in situ powder X-ray diffraction (XRD) method under high pressure and high temperature. The crystals were grown using NaCl–KCl flux at 1350 °C and B_2O_3 flux at 1150 °C. High growth temperature of 1350 °C for the NaCl–KCl flux caused Pt contamination from the crucible and oxygen deficiency for the crystals obtained. The crystal growth using B_2O_3 flux proceeded at lower temperature by grain growth with material transfer through B_2O_3. The crystal obtained was characterized by single-crystal XRD method, and was found to have a stoichiometric composition, $Tl_2Ru_2O_{7-\delta}$ ($\delta = 0$), with a structural phase transition around 120 K. The grain growth technique with B_2O_3 is efficient for high-temperature single-crystal growth under high pressure.

Keywords: Pyrochlore; Single crystal; High-pressure synthesis

1. Introduction

The ruthenium pyrochlores $A_2Ru_2O_7$ exhibit a wide range of physical properties. For instance, $Bi_2Ru_2O_7$ and $Pb_2Ru_2O_{6.5}$ show metallic and Pauli paramagnetic with low electrical resistivities of $10^{-3}\,\Omega$ cm at room temperature [1,2]. While $Ln_2Ru_2O_7$ (Ln = Pr–Lu) and $Y_2Ru_2O_7$ are semiconducting [3]. $Tl_2Ru_2O_{7-\delta}$ shows a metallic–insulator transition (M–I transition) around 120 K [4]. The electronic structures of $Bi_2Ru_2O_7$, $Y_2Ru_2O_7$ and $Pb_2Ru_2O_{6.5}$ have been investigated by XPS, UPS and HREELS [5–7] and by the pseudofunction method [8]. The unoccupied Pb or Bi 6*p* states are close to E_F and play an important role in the metallic conductivity by mixing with the Ru 4*d* state via the framework oxygen.

The thallium pyrochlore, $Tl_2Ru_2O_7$, was first synthesized by Sleight and Bouchard [9] under a pressure of 0.3 GPa and showed metallic properties. Takeda et al. [10] reported that the properties of the thallium ruthenium pyrochlore depended on oxygen content δ in $Tl_2Ru_2O_{7-\delta}$. $Tl_2Ru_2O_{7-\delta}$ showed the M–I transition with a decrease in the magnetic susceptibility at 120 K for $\delta = 0$, metallic–semiconductor transition and spin-glass-like behavior for $\delta = 0.04$, and metallic and paramagnetic behavior for $\delta = 0.29$ [10,11]. The relationships among the composition and electrical and magnetic properties were clarified by the study using polycrystalline pyrochlore samples. Neutron powder diffraction results indicated that a structural transition from cubic to orthorhombic lattice with the Ru and Tl sites located over two sites [12] accompanied the M–I transition.

*Corresponding author. Fax: +81 45 924 5401.
E-mail address: kanno@echem.titech.ac.jp (R. Kanno).

0022-4596/$ - see front matter © 2005 Elsevier Inc. All rights reserved.
doi:10.1016/j.jssc.2005.12.017

On the other hand, Sakai et al. [13] reported that no splitting of Tl site was observed below the M–I transition temperature by Tl-NMR measurements. The relationships between the structure and M–I transition are not clarified by the study using polycrystalline pyrochlore samples, therefore the detailed the mechanism of M–I transition are not still clear. The study based on single crystal is essential to clarify the mechanism of M–I transition. It is, however, difficult to grow single crystals of $Tl_2Ru_2O_7$ pyrochlore, because the material has high melting point and is insoluble in water and any acids. In addition, the oxygen content δ in $Tl_2Ru_2O_{7-\delta}$ is sensitive to the preparation condition and the stoichiometric composition ($\delta = 0$) cannot be obtained under ambient pressure. To solve these problems, the growth of single crystal of $Tl_2Ru_2O_7$ pyrochlore is necessary under high pressure.

High-pressure synthesis has many features, as fields of material preparation can widely extend by an addition to experimental parameter. The method is necessary to prepare high-pressure phase, a useful tool to handle materials having high vapor pressures, and possible to control the redox atmosphere or high oxygen pressure using oxidizing and reducing agents. However, high-pressure synthesis is not conventionally used for single-crystal growth. Because the reaction process cannot be observed, in situ investigations of phase relationship under high pressure and high temperature are difficult, and this also makes it difficult to optimize the experimental conditions suitable for crystal growth.

In the present study, in situ synchrotron X-ray diffraction (XRD) methods have been used to investigate phase relationship at high pressure and high temperature. Based on the direct observations of the reaction process between $Tl_2Ru_2O_7$ and flux materials, single crystals of $Tl_2Ru_2O_7$ pyrochlore were grown at 2–3 GPa.

2. Experimental

The starting materials were Tl_2O_3 (Wako, 99.9%) and RuO_2 (Sumitomo Metal Mining). These were weighed and mixed with KCl, NaCl and B_2O_3 used as the flux agent, and $KClO_4$ and $NaClO_4$ used as oxidization agent. $KClO_4$ and $NaClO_4$ decompose and produce oxygen pressure at high temperature, and then they work as flux agent.

In situ XRD under high pressure was measured by synchrotron X-ray on beam-line 14B1 at SPring-8, Japan Synchrotron Radiation Research Institute. In the case of (i) NaCl–KCl flux, Tl_2O_3, RuO_2, $KClO_4$ and $NaClO_4$ weighed and mixed at the molar ratio of 1.0:2.0:0.5:0.5. In the case of (ii) B_2O_3 flux, Tl_2O_3, RuO_2, B_2O_3 and $KClO_4$ weighed and mixed at the molar ratio of 1.0:2.0:0.5:0.5. The mixtures of about 0.25 g were sealed platinum capsule (ϕ 4 mm × 7 mm). The measurements were performed by means of energy dispersive method using conventional cubic anvil-type high-pressure apparatus installed at beam-line 14B1. White beam X-ray was used to irradiate the sample through the high-pressure cell and was detected with a Ge solid-state detector fixed at $2\theta \approx 4^\circ$. The XRD patterns under high pressure were collected at various temperatures. The sample was pressed at room temperature and then heated stepwise.

Single crystals of $Tl_2Ru_2O_7$ pyrochlore were grown at 2 or 3 GPa using a cubic-type high-pressure apparatus. In the case of (i) NaCl–KCl flux, Tl_2O_3, RuO_2 and KCl, $KClO_4$ and NaCl weighed and mixed at the molar ratio of 1.0:2.0:0.5:0.5:1.0. The molar ratio of flux and oxidization agent was different from that used in synchrotron XRD measurement because oxygen pressure was controlled to avoid blowing out. The molar ratio of potassium and sodium were fixed at 1.0:1.0, a difference of the amount of oxidization agent was a matter of small importance. The mixture about 3.7 g was pressed at 10 MPa and sealed in platinum capsule (ϕ 10 mm × 12 mm). In the case of (ii) B_2O_3 flux, Tl_2O_3, RuO_2 and B_2O_3, $KClO_4$ weighed and mixed at the molar ratio of 1.0:2.0:0.5:0.5. The mixture about 3.4 g was pressed at 10 MPa and sealed in platinum capsule (ϕ 10 mm × 12 mm).

XRD data of a single crystal of $Tl_2Ru_2O_7$ pyrochlore was collected by Rigaku R-AXIS Rapid diffractometer with Imaging-Plate (IP)-type detector using Mo$K\alpha$ radiation at room temperature. Black and octahedral-shaped single crystal of about 0.07 mm in radius was used for the intensity data collection. Cell dimensions were determined using 7891 reflections with a range around $2\theta \approx 140^\circ$. A total of 6875 reflections were observed within the limit of $2\theta \approx 90^\circ$, including averaged 250 independent reflections ($R_{int} = 6.45\%$). X-ray data collection, cell refinement and data reduction were performed using RAPID-AUTO [14]. Absorption correction was made using the program NUMABS [15]. Extinction correction and refinement of structural parameters were performed using SHELXL-97 [16] in Win-GX [17]. An oscillation photograph was taken by the above described IP-type diffractometer at 123 K.

The magnetic susceptibilities were measured in an external magnetic field of 1000 Oe from 5 to 300 K using SQUID magnetometer (Quantum Design, MPMSXL).

3. Results and discussion

3.1. In situ X-ray diffraction measurements under high pressure

Synchrotron XRD was measured from ambient temperature to 1673 K at 2 and 3 GPa. Fig. 1 shows the diffraction patterns for the thallium ruthenium pyrochlore with (i) NaCl–KCl flux at 2 GPa and (ii) B_2O_3 flux at 3 GPa. The extra reflections were observed due to the characteristic radiation of lead (PbKα_2, Kα_1) used as a beam stopper at 72.9 and 75.1 keV, and platinum (PtKα_2, Kα_1) used as the capsule at 65.1 and 66.8 keV. A break in slope near 78 keV corresponded to the absorption edge of Pt. The diffraction patterns at the bottom in both Fig. 1(a) and (b) were taken at room temperature and ambient

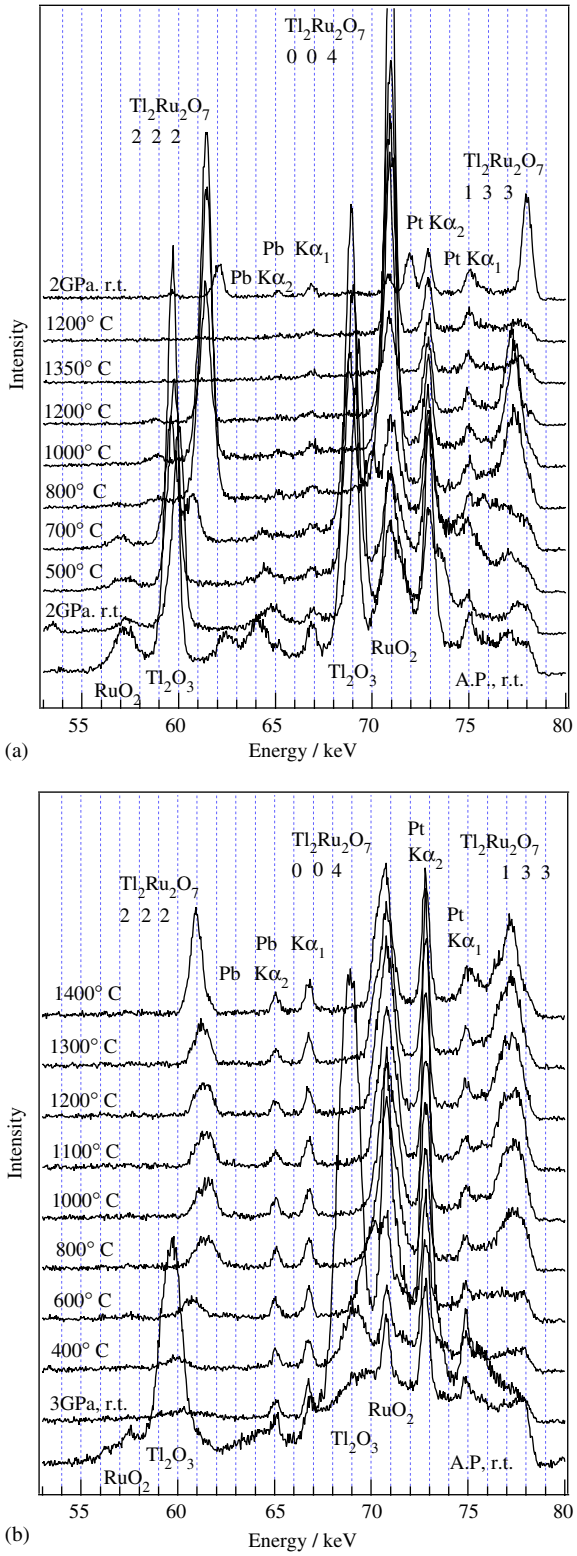

Fig. 1. Synchrotron XRD patterns for $Tl_2Ru_2O_7$ at various temperatures (a) using NaCl–KCl flux at 2 GPa and (b) B_2O_3 flux at 3 GPa.

pressure. The reflections taken under high pressure and at room temperature shifted to the high-energy side, these shifts attributed to lattice contraction under pressure. Another characteristic feature of the patterns at 2–3 GPa is peak broadening, which might be due to lattice strain and/or small particle size of the powders crushed by high pressure. The patterns observed under high pressure and at room temperature could still be identified as being the starting materials.

For the sample using flux (i) shown in Fig. 1(a), the reflections from starting materials, Tl_2O_3, RuO_2, were observed below 600 °C. The peaks shifted slightly to the low-energy side with heating. The reaction started at 700 °C, and then single-phase $Tl_2Ru_2O_7$ pyrochlore observed above 800 °C. $Tl_2Ru_2O_7$ melted at 1350 °C, indicating that single crystals of $Tl_2Ru_2O_7$ pyrochlore could be synthesized by slow cooling from 1350 °C at 2 GPa.

For the flux (ii) shown in Fig. 1(b), the reaction started around 600 °C, and the single-phase $Tl_2Ru_2O_7$ pyrochlore was observed above 800 °C. As the sample was heated the reflections from $Tl_2Ru_2O_7$ pyrochlore shifted to the low-energy side as in the case of (i). The reflections of $Tl_2Ru_2O_7$ pyrochlore were still observed at 1400 °C and $Tl_2Ru_2O_7$ pyrochlore was not melted. However, the recovered sample contained single crystals of $Tl_2Ru_2O_7$ pyrochlore. These suggest that single-crystal growth is not by way of the melting process as in the case of the NaCl–KCl flux. It is assumed that the single-crystal growth was a result of the grain growth with B_2O_3 at lower temperature than that of the NaCl–KCl flux.

3.2. Single-crystal growth

Single crystals of $Tl_2Ru_2O_7$ were grown using the NaCl–KCl flux and the B_2O_3 flux. For the NaCl–KCl flux, the mixture was heated up to 1320 °C in 30 min, held this temperature for 10 min, and then cooled slowly to 1200 °C for 15 h at 2 GPa in a sealed platinum capsule. The sample was then cooled to room temperature in 8 h. The reaction products were a mixture of single crystals of octahedral shape with black and metallic luster ($Tl_2Ru_2O_{7-\delta}$), single crystals with transparent and orange color (K_2PtCl_4), and powders with auburn color (K_2PtCl_4). The black and octahedral-shaped single crystals were obtained with the size of about $0.3 \times 0.3 \times 0.3\,mm^3$. The crystals were determined to be the thallium pyrochlore by powder XRD measurements. However, the magnetic susceptibility for the single crystals showed no anomaly around 120 K [10], which is the same behavior of the thallium pyrochlore with oxygen deficiency, $Tl_2Ru_2O_{7-\delta}$ [10]. Longer heating periods and higher heating temperature caused oxygen deficiency, and no stoichiometric composition could be obtained using the NaCl–KCl flux. The crystals with orange color and the powders with auburn color were identified as K_2PtCl_4 by powder XRD measurements, indicating that the reaction of $Pt \rightarrow Pt^{2+}$ proceeded in the reaction vessel together with the single-crystal formation of the pyrochlore. The oxidation reaction of platinum may explain the oxygen deficiency in $Tl_2Ru_2O_{7-\delta}$ single crystal.

The single crystals were then grown with the B_2O_3 flux. In situ XRD measurements under high pressure indicated that the crystal growth in the B_2O_3 flux proceeded without complete melting of the pyrochlore at lower temperature than the growth from the complete melting at 1350 °C in the NaCl–KCl flux. The sample were heated up to 1150 °C in 30 min, then held this temperature for 20 h and cooled to room temperature for 8 h under 2 GPa. The flux was washed away by water and dilute hydrochloric acid. Single crystals of $Tl_2Ru_2O_7$ were obtained with octahedral shapes and had dimensions of about $0.1 \times 0.1 \times 0.1\,mm^3$. Single crystals of $Tl_2Ru_2O_7$ pyrochlore obtained at the center of the crucible showed no Pt contamination by EDX measurements. Fig. 2 shows the SEM photograph of the single crystal of $Tl_2Ru_2O_7$.

The structure refinement was carried out using XRD for the single-crystal specimen about $0.07 \times 0.07 \times 0.07\,mm^3$ with the space group $Fd\bar{3}m$ (A-227-2) and the pyrochlore structure model, Tl at 16*d* (1/2, 1/2, 1/2), Ru at 16*c* (0, 0, 0) and O(1) at 48*f* (*x*, 1/8, 1/8) with $x \approx 0.32$, and O(2) at 8*b* (3/8, 3/8, 3/8). All the site occupation parameters were fixed at the value of starting composition. In the final refinement, a total of 11 parameters including anisotropic atomic displacement parameter of individual elements were refined. The final *R* factor was 2.10%. The largest residual Fourier peak and hole for final refinement were 1.22 and $-1.34\,e/Å^3$. The crystallographic data, data collection parameters and the refinement results are summarized in Table 1. The structure analysis confirmed the pyrochlore structure.

Fig. 3 shows the X-ray oscillation photograph of the single crystal taken at 123 K. Some extra reflections appeared in addition to the reflections observed at ambient temperature. These reflections were not satisfied the reflection conditions of space group $Fd\bar{3}m$ (A-227-2), *hkl*: $h+k=2n$, $h+l=2n$ and $k+l=2n$. The single crystals obtained by the B_2O_3 flux showed the structural transition and has stoichiometric composition. The structure study of low-temperature phase is currently underway. Table 2 summarizes the selected bond distances and angles together

Table 1
Summary of experimental and crystallographic data for $Tl_2Ru_2O_7$

Chemical formula	$Tl_2Ru_2O_7$
Space group	$Fd\bar{3}m$
Lattice parameter *a* (Å)	10.2145(19)
V (Å^3)	1065.7(3)
Z	8
Calculated density (g/cm^3)	9.011
Crystal size (mm)	Octahedral, $0.07 \times 0.07 \times 0.07$
Maximum 2θ (deg.)	~90
Number of measured reflections	6875
Number of unique reflections	250
R factor (%)	2.10
R_w factor (%)	5.584
Weighting scheme	$1/[\sigma^2(F_o^2)+(0.0155P)^2+0.0000P]$ where $P=(F_o^2+2F_c^2)/3$
Number of refined parameters	11
Goodness of fit	0.618

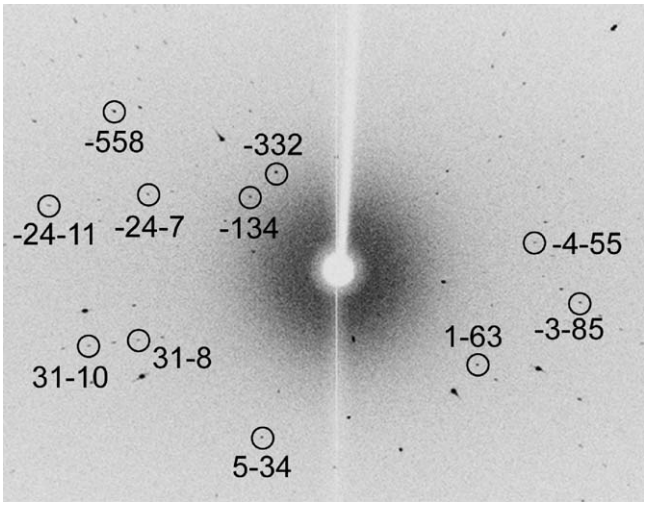

Fig. 3. Oscillation photograph taken at 123 K, showing forbidden reflections in space group $Fd\bar{3}m$.

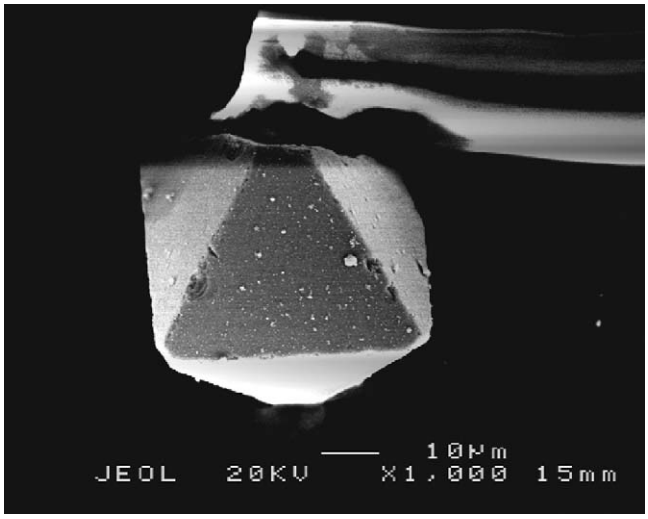

Fig. 2. SEM photograph of a single crystal of $Tl_2Ru_2O_7$ pyrochlore.

Table 2
Interatomic distances and bond angles for $Tl_2Ru_2O_7$ pyrochlore

Sample feature	Single crystal	Powder [10]
Bond distance *d*/Å		
Ru–O	1.967(3)	1.9586(18)
Tl–O(1)	2.531(6)	2.530(3)
Tl–O(2)	2.2115(4)	2.2054(1)
Bond angles θ/°		
Ru–O–Ru	133.3(5)	133.7(2)
Tl–O(1)–Tl	91.0(3)	90.78(15)
O(1)–Ru–O(1)	95.4(3)	95.09(17)

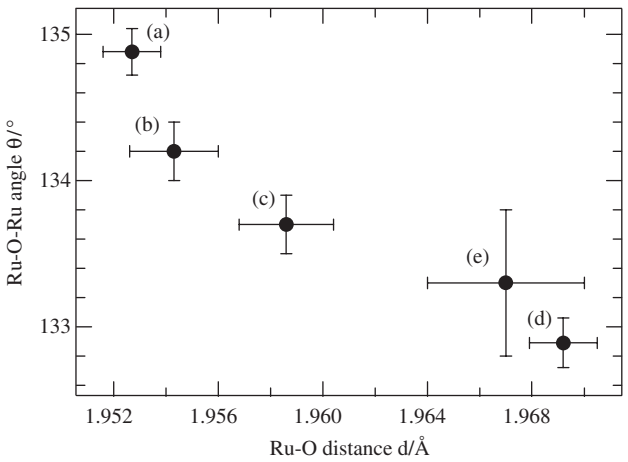

Fig. 4. Relationship between the Ru–O distances and Ru–O(1)–Ru angles: (a) $Tl_2Ru_2O_{6.71}$: high-temperature phase, metallic [11]; (b) $Tl_2Ru_2O_{6.95}$: high-pressure phase, resistivity change around 50 K [10]; (c) $Tl_2Ru_2O_7$: high oxygen pressure phase, metallic–insulator transition around 120 K [10]; (d) $Tl_2Ru_2O_7$: low-temperature phase, semiconducting [11] and (e) $Tl_2Ru_2O_7$ single crystal obtained in this study: growing under high oxygen pressure.

with those reported for $Tl_2Ru_2O_{7-\delta}$ determined by neutron diffraction methods. The distances observed for the single crystal are consistent with those obtained by the powder diffraction data [10]. Fig. 4 shows the relationship between the bond distances and the bond angles obtained both from powder and single-crystal samples. In the neutron diffraction measurements on powdered samples, Ru–O(1) distance increases, Ru–O(1)–Ru angle decreases, and the Tl–O(1) distance decreases with increasing oxygen contents. The Ru–O(1)–Ru angle decreased with increasing Ru–O(1) distance, which indicates small *B*–O–*B* overlap integrals in the pyrochlore structure. The single crystal obtained in the present study showed smaller Ru–O(1)–Ru angle and larger Ru–O(1) distance, which are indications of the stoichiometric oxygen composition.

In the present study, we showed that the flux method using B_2O_3 was quite efficient to grow single crystals at high-pressure and high-temperature conditions. Single-crystal growth under high pressure was previously studied from the melts of the target materials. For example, single-crystal growth and direct observation of the growth conditions under high pressure were reported for the phase transition to high-pressure phase of $(VO)_2P_2O_7$ [18] and congruent melting of GaN [19]. However, high melting points of the thallium pyrochlore in the present study caused a reaction between the crucible and the sample, which made it difficult to control the oxygen content. Lower growth temperatures using B_2O_3 flux made the single crystals having the stoichiometric compositions with no contamination from the crucible. The in situ XRD measurements under high pressure clarified the grain growth mechanism without complete melting of the pyrochlore. This method is efficient for single-crystal growth under high pressure for the samples with high melting points.

4. Conclusion

The growth conditions of the pyrochlore, $Tl_2Ru_2O_7$, were determined by in situ XRD study under high pressure. Our in situ observation was quite efficient to clarify the single-crystal formation process under high oxygen pressure and high temperatures. Two types of growth mechanisms were revealed: crystal growth from the melt, and the grain growth. However, high growth temperature of the former technique caused Pt contamination and oxygen deficiency in the pyrochlore. On the other hand, partially melting on the pyrochlore grain in the B_2O_3 flux causes grain growth, leading to the single-crystal formation. Obtained single crystal of $Tl_2Ru_2O_7$ was confirmed to be stoichiometric by the structural phase transition. We could successfully indicate the new grain-growth technique to synthesize single crystals with high melting point under high oxygen pressure and high temperature conditions.

Acknowledgments

This work was supported by a grant-in-aid from The Ministry of Education, Culture, and Sports, Science and Technology of Japan. The synchrotron radiation experiments were performed at the SPring-8 with the approval of the Japan Synchrotron Radiation Research Institute (Proposal no. 2001B0596ND-np).

Reference

[1] R.J. Bouchard, J.L. Gillson, Mater. Res. Bull. 6 (1971) 669–680.
[2] J.M. Longo, P.M. Raccah, J.B. Goodenough, Mater. Res. Bull. 4 (1969) 191–202.
[3] R. Aléonald, E.F. Bertaut, M.C. Montmory, R. Pauthenet, J. Appl. Phys. 33 (1962) 1205.
[4] H.S. Jarrett, A.W. Sleight, J.F. Weiher, J.L. Gillson, C.G. Frederick, G.A. Jones, R.S. Swingle, D. Swartzfager, J.E. Gulley, P.C. Hoell, in: R.D. Parks (Ed.), Valence Instabilities and Related Narrow-band Penomena, Plenum, New York, 1977, pp. 545–549.
[5] J.B. Goodenough, A. Hamnett, D. Tells, in: H. Fritzsche, D. Alder (Eds.), Localization and Metal–Insulator Transition, Plenum, New York, 1985, p. 161.
[6] P.A. Cox, J.B. Goodenough, P.J. Tavener, D. Telles, R.G. Egdell, J. Solid State Chem. 62 (1986) 360–370.
[7] P.A. Cox, R.G. Egdell, J.B. Goodenough, A. Hamnett, C.C. Naish, J. Phys. C: Solid State Phys. 16 (1983) 6221–6239.
[8] W.Y. Hsu, R.V. Kasowski, T. Miller, T.C. Chiang, Appl. Phys. Lett. 52 (1988) 792–794.
[9] A.W. Sleight, R.J. Bouchard, Solid state chemistry, in: Proceedings of the Fifth Materials Research Symposium, NBS Special Publication, vol. 364, 1972, pp. 227–232.
[10] T. Takeda, M. Nagata, H. Kobayashi, R. Kanno, Y. Kawamoto, M. Takano, T. Kamiyama, F. Izumi, A.W. Sleight, J. Solid State Chem. 140 (1998) 182–193.
[11] R. Kanno, J. Huang, A.W. Sleight, JAERI-M 93-228 2 (1993) 347–354.
[12] T. Takeda, R. Kanno, Y. Kawamoto, M. Takano, F. Izumi, A.W. Sleight, A.W. Hewat, J. Mater. Chem. 9 (1999) 215–222.

[13] H. Sakai, M. Kato, K. Yoshimura, K. Kosuge, J. Phys. Soc. Jpn. 71 (2002) 422–424.
[14] Rigaku, RAPID-AUTO Manual No. MJ13159A01, Rigaku Corporation, 1999.
[15] T. Higashi, NUMABS, Rigaku Corporation, 2000.
[16] G. Sheldrick, SHELX-97, University of Gottingen, 1997.
[17] L.J. Farrugia, J. Appl. Crystallogr. 32 (1999) 837–838.
[18] T. Saito, T. Terashima, M. Azuma, M. Takano, T. Goto, H. Ohta, W. Utsumi, P. Bordet, D.C. Johnston, J. Solid State Chem. 153 (2000) 124–131.
[19] W. Utsumi, H. Saitoh, H. Kaneko, T. Watanuki, K. Aoki, O. Shimomura, Nat. Mater. 2 (2003) 735–738.